PHYSICAL REVIEW B **88**, 081203(R) (2013)

Diluted ferromagnetic semiconductor Li(Zn,Mn)P with decoupled charge and spin doping

Z. Deng,[1] K. Zhao,[1] B. Gu,[2] W. Han,[1] J. L. Zhu,[1] X. C. Wang,[1] X. Li,[1] Q. Q. Liu,[1] R. C. Yu,[1] T. Goko,[3] B. Frandsen,[3] L. Liu,[3] Jinsong Zhang,[4] Yayu Wang,[4] F. L. Ning,[5] S. Maekawa,[2] Y. J. Uemura,[3] and C. Q. Jin[1,*]

[1]*Beijing National Laboratory for Condensed Matter Physics and Institute of Physics, Chinese Academy of Sciences, Beijing 100190, China*

[2]*Advanced Science Research Center, Japan Atomic Energy Agency, Tokai 319-1195, CREST, Japan Science and Technology Agency, Sanbancho, Tokyo 102-0075, Japan*

[3]*Department of Physics, Columbia University, New York, New York 10027, USA*

[4]*Department of Physics, Tsinghua University, Beijing 100084, China*

[5]*Department of Physics, Zhejiang University, Hangzhou 310027, China*

(Received 21 April 2013; published 21 August 2013)

We report the discovery of a diluted magnetic semiconductor, Li(Zn,Mn)P, in which charge and spin are introduced independently via lithium off-stoichiometry and the isovalent substitution of Mn^{2+} for Zn^{2+}, respectively. Isostructural to (Ga,Mn)As, Li(Zn,Mn)P was found to be a *p*-type ferromagnetic semiconductor with excess lithium providing charge doping. First-principles calculations indicate that excess Li is favored to partially occupy the Zn site, leading to hole doping. Ferromagnetism with Curie temperature up to 34 K is achieved while the system still shows semiconducting transport behavior.

DOI: 10.1103/PhysRevB.88.081203 PACS number(s): 75.50.Pp, 75.50.Dd, 75.30.Kz

I. INTRODUCTION

Spintronic devices utilize the electron's charge and spin degrees of freedom to achieve novel quantum functionalities. Diluted magnetic semiconductors (DMS) constitute an important category of spintronic materials that have the potential to be successfully incorporated into the existing semiconductor industry. The prototypical DMS (Ga,Mn)As,[1] discovered in the 1990s, accomplishes spin and charge doping simultaneously through the heterovalent substitution of the magnetic ion Mn^{2+} for Ga^{3+}. Two challenges have presented themselves in this material. First, the heterovalent nature of this "integrated spin/charge" doping results in severely limited chemical solubility in (Ga,Mn)As, restricting specimen fabrication to metastable thin films by molecular beam epitaxy; second, the simultaneous spin and charge doping precludes the possibility of individually tuning the spin and charge degrees of freedom.

A new type of ferromagnetic DMS that overcomes both of these challenges was recently discovered.[2] Li(Zn,Mn)As utilizes excess Li concentration to introduce hole carriers, while independently making the isovalent substitution of Mn^{2+} for Zn^{2+} to achieve local spin doping. With no heterovalent substitutions to restrict chemical solubility, bulk specimens of Li(Zn,Mn)As were successfully fabricated.[2] Shortly thereafter, another new bulk ferromagnetic DMS with independent charge and spin doping, $(Ba,K)(Zn,Mn)_2As_2$, was found with Curie temperature (T_C) up to 180 K. Holes are doped via (Ba^{2+}, K^{1+}) substitution, while spins are introduced by isovalent (Zn^{2+}, Mn^{2+}) substitution.[3] These new DMS materials have the added advantage of being structurally very similar to the recently discovered iron-pnictide high-temperature superconductors, opening up the possibility of creating novel junctions between superconducting, semiconducting, and magnetic materials.

It is noted that previously DMS are successfully obtained on II-VI based compounds conducted such as (Zn,Mn)Te, (Cd,Mn)Te,[4,5] in which the valence of group II cations is identical to that of doped magnetic element Mn, resulting in precise DMS properties. One drawback of Li(Zn,Mn)As is its use of the toxic element As. In the present work, we report the synthesis of a DMS in which As has been replaced by nontoxic P as shown in Fig. 1(a). We found that Li(Zn,Mn)P exhibits soft ferromagnetic behavior with a relative lower carrier density than those for Li(Zn,Mn)As and (Ga,Mn)As,[2,6–8] but with comparable T_C, offering the advantage of much improved semiconductive behavior and the potential for higher T_C via increased carrier concentration.

II. EXPERIMENT

Polycrystalline specimens were prepared as described in Refs. 2 and 3. High-purity starting materials with molar amounts proportional to the nominal element concentrations were pressed into a pellet and loaded into a Ta tube with high-purity argon. The Ta tube, which prevented the evaporation of Li, was then sealed into an evacuated quartz tube. All procedures were performed in a glove box under high-purity argon atmosphere. The samples were heated to 900 °C and held for several days before the temperature was slowly decreased. The specimens were characterized by x-ray powder diffraction on a PANalytical X'Pert diffractometer operating with Cu $K\alpha$ radiation. Lattice parameters were determined via Rietveld analysis using the GSAS software package. The real atomic ratios of heavy elements such as Zn, Mn, or As measured from energy dispersive analysis of x-ray (EDAX) are nearly the same as the nominal ones, such as those for Mn:(Zn + Mn), which are about 0.032, 0.051, and 0.074 for nominal $Li_{1.02}(Zn_{0.97}Mn_{0.03})P$, $Li_{1.02}(Zn_{0.95}Mn_{0.05})P$, and $Li_{1.02}(Zn_{0.93}Mn_{0.07})P$, respectively. It is rather difficult to measure Li concentration since it is a very light element. But its concentration evolution can be inferred from lattice parameter change. Successful Li and Mn doping are supported by continuing lattice constant increasing as shown in Fig. 1(b). The concentrations of Li and Mn in the paper therefore use the nominal composition. dc-magnetization measurements were performed on a Quantum Design Superconducting Quantum Interference Device-Vibrating Sample

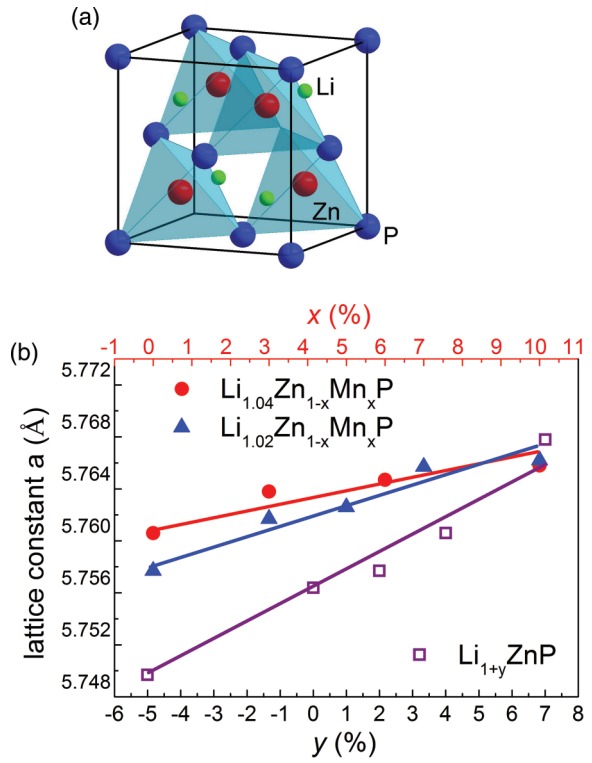

FIG. 1. (Color online) (a) Crystal structure of LiZnP showing $[ZnP_4]$ tetrahedral coordination. (b) Lattice constants of $Li_{1+y}ZnP$, $Li_{1.02}Zn_{1-x}Mn_xP$, and $Li_{1.04}Zn_{1-x}Mn_xP$ for various Li and Mn concentrations. The systematic change of lattice parameters indicates the successful substation of the elements.

Magnetometer (SQUID-VSM). Resistivity and Hall effect measurements were carried out on a Quantum Design Physical Property Measurement System (PPMS) using the four-probe method and the Hall bar method, respectively.

III. RESULTS AND DICUSSION

A. Experimental results

Step-scanning powder x-ray diffraction measurements showed that pristine LiZnP crystallizes into a structure similar to zinc-blende-type GaAs with space group $F\bar{4}3m$,[2] as shown in Fig. 1(a). The refined lattice parameter of LiZnP is $a = 5.7564$ Å.[9,10] We found that chemically stable bulk crystals of $Li_{1+y}(Zn_{1-x}Mn_x)P$ can be obtained for excess Li with $y \leqslant 0.15$ and Mn concentrations x up to at least 0.1. As shown in Fig. 1(b), the lattice parameter evolved systematically with Li and Mn concentrations, suggesting successful chemical doping.

The temperature-dependent magnetization $M(T)$ and field-dependent magnetization $M(H)$ were measured for $Li_{1+y}(Zn_{1-x}Mn_x)P$ with $-0.05 \leqslant y \leqslant 0.07$ and $x = 0$, 0.03, 0.06, and 0.1. The specimens with deficient Li showed spurious weak ferromagnetic signals above room temperature caused by the ferromagnetic impurity MnP.[11] Specimens with excess Li, on the other hand, demonstrated robust ferromagnetism, as displayed in Fig. 2. Figure 2(a) shows $M(T)$ for $Li_{1.04}(Zn_{1-x}Mn_x)P$ specimens, $x = 0$, 0.03, 0.06, and 0.1, in an applied field of 100 Oe in both zero-field-cooling

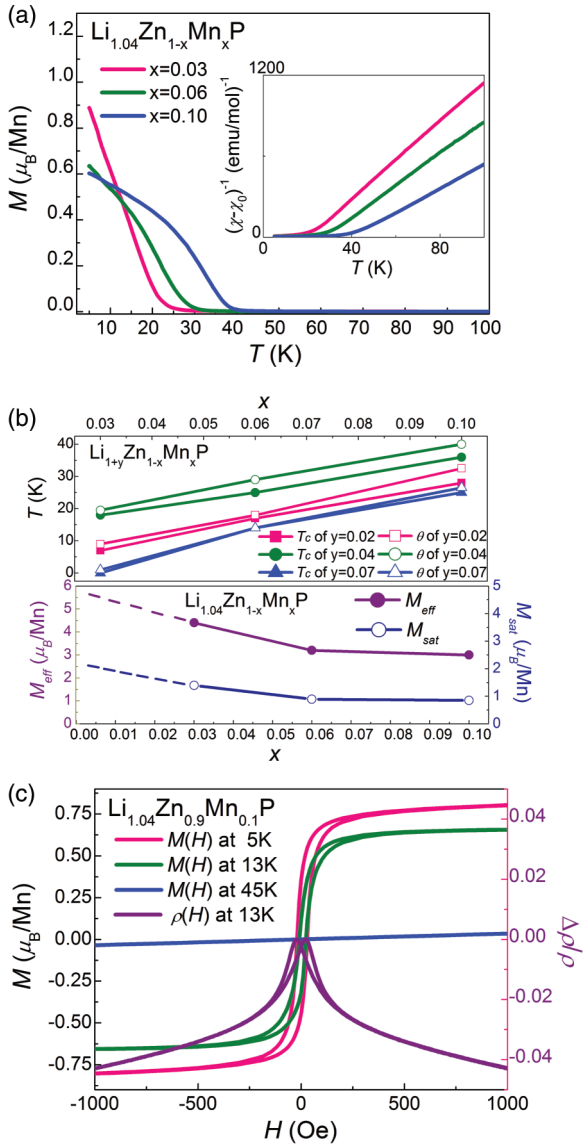

FIG. 2. (Color online) dc-magnetization measurements of Li(Zn,Mn)P systems. (a) $M(T)$ curves in ZFC and FC modes with $H = 100$ Oe for $Li_{1.04}(Zn_{1-x}Mn_x)P$ specimens (no visible difference between ZFC and FC procedures for small coercive fields). Inset shows the temperature dependence of the inverse susceptibility. (b) Top: T_C and θ for $Li_{1+y}Zn_{1-x}Mn_xP$. Bottom: $M_{\rm eff}$ and $M_{\rm sat}$ for $Li_{1.04}Zn_{1-x}Mn_xP$. Dashed lines indicate extrapolation. (c) $M(H)$ and $\rho(H)$ in $Li_{1.04}Zn_{0.9}Mn_{0.1}P$ show hysteresis, demonstrating ferromagnetism with a small coercive field of about 50 Oe.

(ZFC) and field-cooling (FC) modes. T_C, determined by the projected line method, clearly increases up to 34 K, as shown in Fig. 2(b). Above T_C, the susceptibility χ can be fit to Curie-Weiss law [Figs. 2(a) and 2(b)], $(\chi - \chi_0)^{-1} = (T - \theta)/C$, where χ_0 is a temperature-independent term, C is the Curie constant, and θ is the Weiss temperature. The positive value of θ found for $Li_{1.04}(Zn_{1-x}Mn_x)P$ [Fig. 2(b)] indicates a ferromagnetic interaction between Mn^{2+} ions.

The effective paramagnetic moment ($M_{\rm eff}$) obtained from the Curie constant [solid purple circles in Fig. 2(b)] decreases with increasing Mn doping, a trend also found in other systems doped with magnetic ions.[12–14] Extrapolation of $M_{\rm eff}$

to lower Mn concentrations yields a value of approximately $5.9\mu_B$/Mn, as expected for the fully high-spin oriented Mn^{2+} ion. Figure 2(b) also shows the saturation moment per Mn (M_{sat}) in an applied field of 500 Oe, found to be about 1–2μ_B/Mn. For ferromagnetic (Ga,Mn)As, Li(Zn,Mn)As, and (Ba,K)(Zn,Mn)$_2$As$_2$, M_{sat} are about 2–4μ_B/Mn,[15] 1–3μ_B/Mn,[2] and 1–2μ_B/Mn,[3] respectively, which are comparable to that of Li(Zn,Mn)P. As M_{eff}, M_{sat} decreases with increasing Mn concentration, likely due to competition between antiferromagnetic coupling of nearest neighbor Mn moments and ferromagnetic coupling of Mn moments mediated by the doped hole carriers. Figure 2(c) shows the hysteresis curves for $Li_{1.04}Zn_{0.9}Mn_{0.1}P$, indicating soft ferromagnetic behavior with a very small coercive field (H_C) of ~50 Oe.

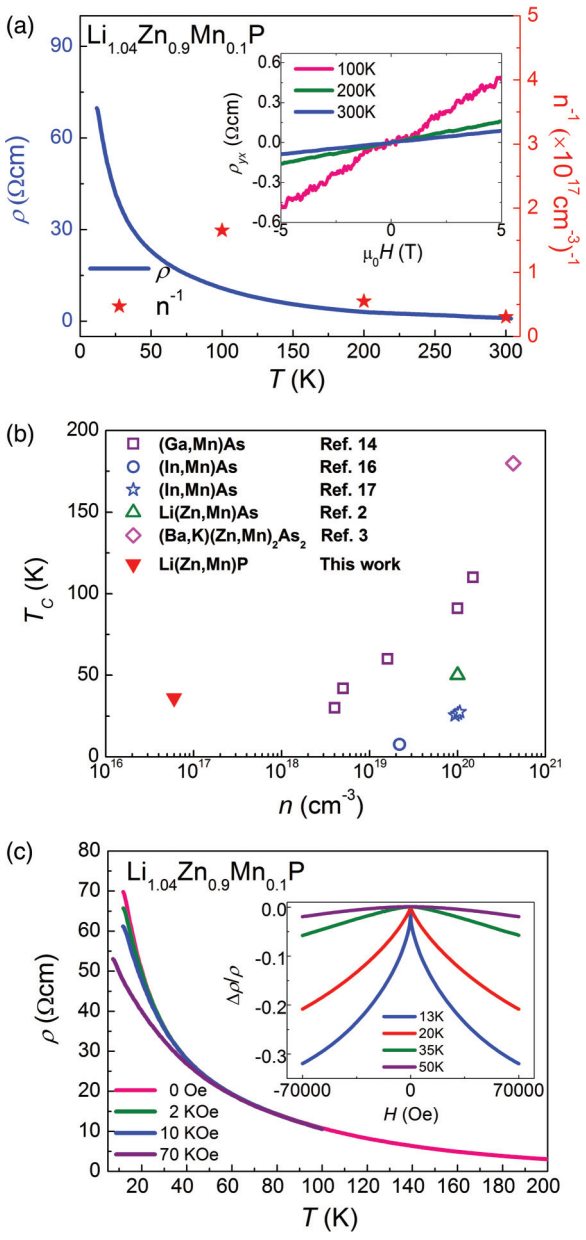

FIG. 3. (Color online) (a) $\rho(T)$ and the inverse carrier concentration for $Li_{1.04}Zn_{0.9}Mn_{0.1}P$. Inset shows Hall resistivity of $Li_{1.04}Zn_{0.9}Mn_{0.1}P$, exhibiting p-type carriers with $n_p = 6.1 \times 10^{16}$ cm^{-3}, 1.82×10^{17} cm^{-3}, and 3.27×10^{17} cm^{-3} at 100, 200, and 300 K, respectively. (b) Correlation between T_C and the hole concentration for four types of tetrahedrally coordinated DMS systems. It exhibits a large difference between Li(Zn,Mn)P and other tetrahedrally coordinated systems. The blue stars represent (In,Mn)As films with electric-field controlled hole concentration. (c) Magnetoresistivity $\rho_H(T)$ of $Li_{1.04}Zn_{0.9}Mn_{0.1}P$ under various field strengths. Inset shows negative magnetoresistance at low temperature.

LiZnP was reported to be a semiconductor with a direct band gap around 2.04 eV.[9] Figure 3(a) shows the resistivity and carrier concentration of $Li_{1.04}Zn_{0.9}Mn_{0.1}P$ from 5–300 K. The resistivity value was diverging and too large at low temperature. Any small misalignment of the two Hall contacts would pick up a longitudinal resistivity signal and this brought large trouble in the Hall effect measurement. As shown in the inset of Fig. 3(a), even a 100 K Hall curve became difficult for measurement. Therefore no anomalous Hall effect signal was detected so far because of technical problems. However, Hall effect measurement of relative high temperature already told us the carrier type and concentration. The conclusion that ferromagnetic order was achieved while the system still shows semiconducting transport behavior is what we can present in this Rapid Communication. Nevertheless, this Rapid Communication just reports the first step of the DMS material. A higher quality sample such as single crystal and high-quality epitaxial film which we are working on will solve the problem.

As plotted in Fig. 3(a), the resistivity obviously increases with decreasing temperature, whereas the mobile hole concentration decreases. This is indicative of typical semiconducting behavior. Somewhat surprisingly, $Li_{1+y}(Zn,Mn)P$, $0 < y < 0.7$, is found to exhibit p-type behavior, not the n-type behavior that one would expect assuming that excess Li provides additional electrons. This is explained by first-principles calculations, which indicate that the excess Li^{1+} ions are thermodynamically favored to occupy the Zn^{2+} sites (see the following section), thereby rendering Li(Zn,Mn)P a p-type DMS.

Previous studies of $(Ga_{1-x}Mn_x)As$ demonstrated that for $0.012 \leqslant x \leqslant 0.03$, ferromagnetic order can be achieved in the full volume fraction while the system still shows semiconducting transport behavior,[15] implying that the paramagnetic to ferromagnetic quantum transition occurs at a different charge/spin concentration than the semiconductor to metal quantum transition. The present work confirms the same situation for Li(Zn,Mn)P. The hole concentration calculated from Hall effect measurements of charge/spin codoped $Li_{1.04}Zn_{0.9}Mn_{0.1}P$ [inset of Fig. 3(a)] is larger than that of pristine LiZnP by more than a factor of 10, but still results in semiconducting transport behavior.[9] Nonetheless, this small hole concentration is evidently sufficient to mediate ferromagnetic coupling of the dilute Mn moments and induce magnetic order. It is likely that the doped holes are not fully delocalized but have sufficient spread in real space to mediate magnetic coupling between neighboring Mn spins, thereby facilitating the buildup of a percolating magnetic network.

Figure 3(b) compares the hole concentrations and ferromagnetic transition temperatures of Li(Zn,Mn)P to those of other DMS systems. The hole concentration of $Li_{1.04}Zn_{0.9}Mn_{0.1}P$ is more than two orders of magnitude smaller than that of typical metallic DMS ferromagnets.[2,3,14,16,17] The relationship between hole concentration and T_C exhibited by the other systems suggests that further charge and spin doping would

TABLE I. Formation energy for excess Li atom at different sites, obtained by DFT calculations. By Ref. 25, the formation energy is given by $E_{\text{formation}} = E_T - n_{\text{Li}}\mu_{\text{Li}} - n_{\text{Zn}}\mu_{\text{Zn}} - n_{\text{P}}\mu_{\text{P}}$, where E_T is the total energy of the supercell, n_x is the number of x atoms in the supercell, and μ_x is the atomic chemical potential. It has $\mu_{\text{Li}} + \mu_{\text{Zn}} + \mu_{\text{P}} = \mu_{\text{LiZnP(bulk)}}$. Table I shows formation energy for two extreme conditions, i.e., the Li-rich plus Zn-rich limits ($\mu_{\text{Li}} = \mu_{\text{Li(bulk)}}$, $\mu_{\text{Zn}} = \mu_{\text{Zn(bulk)}}$) and the Li-rich plus P-rich limit ($\mu_{\text{Li}} = \mu_{\text{Li(bulk)}}$, $\mu_{\text{P}} = \mu_{\text{P(bulk,black)}}$). The experimental condition can be between these two extreme conditions.

LiZnP with excess Li	Formation energy (Li-rich and Zn-rich limits)	Formation energy (Li-rich and P-rich limits)
Interstitial Li (supercell $Li_{28}Zn_{27}P_{27}$)	2.67 eV	2.67 eV
Li at Zn site and Zn is removed (supercell $Li_{28}Zn_{26}P_{27}$)	0.45 eV	−0.93 eV

cause Li(Zn,Mn)P to become metallic and magnetically order at a higher T_C.[18–22] We are currently working on optimizing the materials processing to show this behavior.

Magnetotransport measurements performed on $Li_{1.04}Zn_{0.9}Mn_{0.1}P$ are shown in Fig. 3(c). Several types of effects can produce a magnetoresistance in magnetic semiconductors. Under many conditions, negative magnetoresistance results from the reduction of spin-dependent scattering by aligning the spins in the applied field.[1,14] However, as shown in Figs. 2(c) and 3(c), the negative magnetoresistance is far from saturation in rather high magnetic field, in which spin orientation is fully aligned. In this condition, the negative magnetoresistance is presumably from the weak localization effects.[23] No signature of a metal-insulator phase transition could be found at the Curie point.[15,16,24] The resistivity ρ increases monotonically with decreasing temperature, showing a rapid rise below T_C. Hysteresis is observed in $\rho(H)$ for low fields (∼50 Oe) and low temperatures, corresponding closely to the behavior of the magnetization $M(H)$ [see Fig. 2(c)].

B. Theoretical analysis

We studied the electronic state in Li(Zn,Mn)P with excess Li. We found that (i) for the compound the excess Li atoms prefer to occupy Zn-substitutional sites Li_{Zn}, and thus create the p-type carriers; (ii) the ferromagnetic correlations between Mn ions develop for the case of p-type carriers, and the corresponding effective exchange constant is smaller in Li(Zn,Mn)P than that in Li(Zn,Mn)As and leads to lower Curie temperature.

To study the stable state for excess Li atoms in the Li(Zn,Mn)P compound, we calculated the electronic structures by using the density functional theory (DFT) implemented in the code QUANTUM ESPRESSO.[25] The exchange-correlation interactions are described by the Perdew-Burke-Ernzerhof generalized gradients approximation (GGA), and the electron-ion interactions are represented by the Vanderbilt ultrasoft pseudopotentials. We calculate the formation energy for the interstitial site Li_I and the Zn-substitutional site Li_{Zn}, respectively. Since Mn at Zn-substitutional sites Mn_{Zn} do not introduce any carriers, we study the excess Li in LiZnP. Excess Li atom at interstitial sites Li_I contributes one electron, while Li_{Zn} contributes one hole to the system. Our DFT calculations show that Li_{Zn} makes the formation energy lower than the Li_I case as shown in Table I. It means the carriers will be holes.

To study the magnetic correlations between Mn in Li(Zn,Mn)P, we take the two-step calculations by our combined DFT + QMC (quantum Monte Carlo) method.[26,27] First, the one-particle parts of the Anderson impurity model are formulated within the DFT for determining the host band structure and the impurity-host hybridization. Second, the correlation parts of the Anderson impurity model at finite temperatures are calculated by the QMC method. The calculation details will be published elsewhere.[28] In p-type Li(Zn,Mn)P, ferromagnetic correlations between Mn impurities are obtained by our QMC calculations. In addition, we find that the effective exchange coupling in Li(Zn,Mn)P is smaller than that in Li(Zn,Mn)As.[29] By simple molecular-field theory, larger T_C is expected for larger exchange coupling. This may be the reason why a lower Curie temperature is obtained in Li(Zn,Mn)P than that in Li(Zn,Mn)As.

IV. CONCLUSIONS

In summary, a bulk diluted magnetic semiconductor Li(Zn,Mn)P was successfully synthesized with decoupled spin and charge doping. Li(Zn,Mn)P is a soft magnet with a relatively small coercive field. Ferromagnetic order arises with semiconducting transport behavior, indicating the potential to further enhance T_C with more itinerant carriers. This new DMS will contribute to the further development of new semiconductor materials and spintronic devices based on the individual tuning of spin and charge.

ACKNOWLEDGMENTS

This work was funded by the Chinese NSF and Ministry of Science and Technology (MOST) through research projects; the US NSF PIRE (Partnership for International Research and Education: OISE-0968226) and DMR-1105961 projects at Columbia; the JAEA Reimei project at IOP, Columbia, PSI, McMaster and TU Munich; and NSERC and CIFAR at McMaster.

*Jin@iphy.ac.cn

[1] H. Ohno, Science **281**, 951 (1998).

[2] Z. Deng, C. Q. Jin, Q. Q. Liu, X. C. Wang, J. L. Zhu, S. M. Feng, L. C. Chen, R. C. Yu, C. Arguello, T. Goko, F. Ning, J. Zhang, Y. Wang, a a Aczel, T. Munsie, T. J. Williams, G. M. Luke, T. Kakeshita, S. Uchida, W. Higemoto, T. U. Ito, B. Gu, S. Maekawa, G. D. Morris, and Y. J. Uemura, Nat. Commun. **2**, 422 (2011).

[3] K. Zhao, Z. Deng, X. C. Wang, W. Han, J. L. Zhu, X. Li, Q. Q. Liu, R. C. Yu, T. Goko, B. Frandsen, L. Liu, F. Ning, Y. J. Uemura, H. Dabkowska, G. M. Luke, H. Luetkens, E. Morenzoni, S. R.

Dunsiger, A. Senyshyn, P. Böni, and C. Q. Jin, Nat. Commun. **4**, 1442 (2013).

[4]D. Ferrand, J. Cibert, C. Bourgognon, S. Tatarenko, A. Wasiela, G. Fishman, A. Bonanni, H. Sitter, S. Kolesnik, J. Jaroszynski, A. Barcz, and T. Dietl, J. Cryst. Growth **214-215**, 387 (2000).

[5]A. Haury, A. Wasiela, A. Arnoult, J. Cibert, S. Tatarenko, T. Dietl, and Y. M. d'Aubigné, Phys. Rev. Lett. **79**, 511 (1997).

[6]K. Kuriyama and F. Nakamura, Phys. Rev. B **36**, 4439 (1987).

[7]K. Kuriyama, T. Kato, and K. Kawada, Phys. Rev. B **49**, 11452 (1994).

[8]H. Ohno, A. Shen, F. Matsukura, A. Oiwa, A. Endo, S. Katsumoto, and Y. Iye, Appl. Phys. Lett. **69**, 363 (1996).

[9]K. Kuriyama, T. Katoh, and N. Mineo, J. Cryst. Growth **108**, 37 (1991).

[10]R. Bacewicz and T. F. Ciszek, Appl. Phys. Lett. **52**, 1150 (1988).

[11]Y. Shapira, N. F. Oliveira, C. C. Becerra, and S. Foner, Phys. Rev. B **29**, 361 (1984).

[12]J. M. D. Coey, M. Venkatesan, and C. B. Fitzgerald, Nat. Mater. **4**, 173 (2005).

[13]Y. S. Hor, P. Roushan, H. Beidenkopf, J. Seo, D. Qu, J. G. Checkelsky, L. A. Wray, D. Hsieh, Y. Xia, S.-Y. Xu, D. Qian, M. Z. Hasan, N. P. Ong, A. Yazdani, and R. J. Cava, Phys. Rev. B **81**, 195203 (2010).

[14]F. Matsukura, H. Ohno, A. Shen, and Y. Sugawara, Phys. Rev. B **57**, R2037 (1998).

[15]S. R. Dunsiger, J. P. Carlo, T. Goko, G. Nieuwenhuys, T. Prokscha, A. Suter, E. Morenzoni, D. Chiba, Y. Nishitani, T. Tanikawa, F. Matsukura, H. Ohno, J. Ohe, S. Maekawa, and Y. J. Uemura, Nat. Mater. **9**, 299 (2010).

[16]H. Ohno, H. Munekata, T. Penney, S. von Molnár, and L. L. Chang, Phys. Rev. Lett. **68**, 2664 (1992).

[17]H. Ohno, D. Chiba, F. Matsukura, T. Omiya, E. Abe, T. Dietl, Y. Ohno, and K. Ohtani, Nature (London) **408**, 944 (2000).

[18]T. Dietl, H. Ohno, F. Matsukura, J. Cibert, and D. Ferrand, Science **287**, 1019 (2000).

[19]T. Jungwirth, J. Sinova, J. Masek, J. Kucera, and A. H. MacDonald, Rev. Mod. Phys. **78**, 809 (2006).

[20]T. Dietl, H. Ohno, and F. Matsukura, Phys. Rev. B **63**, 195205 (2001).

[21]D. Chiba, A. Werpachowska, M. Endo, Y. Nishitani, F. Matsukura, T. Dietl, and H. Ohno, Phys. Rev. Lett. **104**, 106601 (2010).

[22]T. Dietl, Nat. Mater. **9**, 965 (2010).

[23]F. Matsukura, M. Sawicki, T. Dietl, D. Chiba, and H. Ohno, Physica E **21**, 1032 (2004).

[24]H. Ohno, J. Magn. Magn. Mater. **200**, 110 (1999).

[25]P. Giannozzi, S. Baroni, N. Bonini, M. Calandra, R. Car, C. Cavazzoni, D. Ceresoli, G. L. Chiarotti, M. Cococcioni, I. Dabo, A. Dal Corso, S. de Gironcoli, S. Fabris, G. Fratesi, R. Gebauer, U. Gerstmann, C. Gougoussis, A. Kokalj, M. Lazzeri, L. Martin-Samos, N. Marzari, F. Mauri, R. Mazzarello, S. Paolini, A. Pasquarello, L. Paulatto, C. Sbraccia, S. Scandolo, G. Sclauzero, A. P. Seitsonen, A. Smogunov, P. Umari, and R. M. Wentzcovitch, J. Phys.: Condens. Matter **21**, 395502 (2009).

[26]B. Gu, N. Bulut, T. Ziman, and S. Maekawa, Phys. Rev. B **79**, 024407 (2009).

[27]J. Ohe, Y. Tomoda, N. Bulut, R. Arita, K. Nakamura, and S. Maekawa, J. Phys. Soc. Jpn. **78**, 083703 (2009).

[28]B. Gu, T. Ziman, and S. Maekawa (unpublished).

[29]S. B. Zhang and J. E. Northrup, Phys. Rev. Lett. **67**, 2339 (1991).